arXiv:1406.7071v2 [hep-ph] 12 Jul 2014

Reaction $\bar{p}p \to \bar{\Lambda}_c^- \Lambda_c^+$ within an effective Lagrangian model

R. Shyam[1] and H. Lenske[2]

[1]*Saha Institute of Nuclear Physics, 1/AF Bidhan Nagar, Kolkata 700064, India and Physics Department, Indian Institute of Technology, Roorkee 247667, India* [a] *and*

[2]*Institut für Theoretische Physik, Universität Gieseen, Heinrich-Buff-Ring 16, D-35392 Giessen, Germany*

(Dated: July 15, 2014)

Abstract

We study the charmed baryon production reaction $\bar{p}p \to \bar{\Lambda}_c^- \Lambda_c^+$ using the t-channel D^0 and D^{*0} meson-exchange diagrams within an effective Lagrangian model involving the physical hadron masses and the coupling constants determined from SU(4) flavor symmetry. The initial and final state distortion effects are accounted for by using a simple eikonal approximation-based procedure. The vertex parameters of our model have been checked by employing them to calculate the cross sections for the $\bar{p}p \to \bar{\Lambda}\Lambda$ reaction within a similar model. We predict the $\bar{\Lambda}_c^- \Lambda_c^+$ production cross sections in the range of $1-30\,\mu b$ for antiproton beam momenta varying between threshold and 20 GeV/c. The respective roles of D^0 and D^{*0} meson exchanges and also those of the vector and tensor components of the D^{*0} coupling have been investigated.

PACS numbers: 13.75.Cs, 14.20.Lq, 11.10.Ef

[a] E-mail: radhey.shyam@saha.ac.in

I. INTRODUCTION

The heavy hadrons consisting of a charm quark are quite distinct in their properties from the light flavored hadrons composed of up (u), down (d), and strange (s) quarks. The presence of the heavy quark in heavy flavor hadrons provides an additional handle for the understanding of quantum chromodynamics (QCD), the fundamental theory of the strong interaction. The large mass of the charm quark introduces a mass scale much larger than the confinement scale $\Lambda_Q \approx 300$ MeV. In contrast, the energy scale of the lighter quarks is $\ll \Lambda_Q$. The presence of two scales in such systems naturally leads to the construction of an effective theory where one can actually calculate a big portion of the relevant physics using perturbation theory and renormalization-group techniques. The heavy quark effective theory (HQET) is one such approach. New symmetry properties, not apparent in QCD, appear in HQET [1–5]. The charm hadrons are ideal candidates to test and apply the predictions of HQET.

In this context, the investigation of the production of heavy flavor hadrons is of great interest. Since the discovery of J/ψ in 1974 [6, 7], the production of charmonium ($c\bar{c}$) states has been extensively studied experimentally in hadroproduction (Tevatron)(see, eg. the reviews [8, 9]), photo- and electro-production (HERA) (see, e.g., Refs. [10, 11] for details) and e^-e^+ annihilation (*BABAR*, Belle, and BES) (see, e.g., Refs. [12–14] for recent reviews) reactions. There are also a large number of theoretical studies of the charmonium production (see, e.g., Ref. [15] for a review). These studies have contributed substantially to enhance our understanding of the charm meson states, their spectroscopy, and decays.

The first charmed baryon states were detected in 1975 in neutrino interactions [16]. Since then, many new excited charmed baryon states have been discovered by the CLEO [17], *BABAR* [18], and Belle [19] facilities (Ref. [5] provides a good review of the older studies). However, the production and spectroscopy of the charmed baryons have not been explored in the same detail as the charmonium states, although they can provide similar information about the quark confinement mechanism. In fact, due to the presence of three quarks (two light and one heavy), the structure of the charmed baryon is more intriguing and complicated. In contrast to mesons, there can be more states as there are more possibilities of orbital excitations.

Most of the current experimental information about the production of the ground state charmed baryon [$\Lambda_c(2286)$] has been derived from the electron-positron annihilation experiments. In the near future, charmed baryon production will be studied in the proton-antiproton ($p\bar{p}$) annihilation

using the "antiproton annihilation at Darmdtadt" ($\bar{P}ANDA$) experiment at the Facility for Antiproton and Ion Research (FAIR) in GSI, Darmstadt (see, e.g., Ref. [20]). The advantage of using antiprotons in the study of the charmed baryon is that in $p\bar{p}$ collisions the production of extra particles is not needed for charm conservation, which reduces the threshold energy as compared to, say, pp collisions. The beam momenta of antiprotons in this experiment will be well above the threshold (10.162 GeV/c) of the $\bar{p}p \to \bar{\Lambda}_c^- \Lambda_c^+$ reaction. For the planning of this experiment, reliable theoretical estimates of the cross section of this reaction would be of crucial importance.

Several authors have calculated the cross section of this reaction by using a variety of models [21–27]. However, the magnitudes of the predicted cross sections are strongly model dependent – they differ from each other by several orders of magnitudes. Furthermore, there is no unanimity about the degrees of freedom to be used in order to describe this reaction. In Ref. [24], the $\bar{p}p \to \bar{\Lambda}_c^- \Lambda_c^+$ reaction has been described within a handbag approach where the amplitude is calculated by convolutions of hard subprocess kernels (representing the process $u\bar{u} \to c\bar{c}$) and the generalized parton distributions, which represent the soft nonperturbative physics. This approach bears some resemblance to the quark-diquark picture used by some of these authors in Ref. [21] to make predictions for the cross sections of the $\bar{\Lambda}_c^- \Lambda_c^+$ production. In the study reported in Ref. [22], a quark-gluon string model together with Regge asymptotics for hadron amplitudes has been used. Calculations reported in Refs. [23, 27] are also based on similar ideas.

On the other hand, in Refs. [25, 26], a meson-exchange model was used to describe the $\bar{p}p \to \bar{\Lambda}_c^- \Lambda_c^+$ reaction. This approach is based on the Jülich meson-baryon model that was employed earlier [28, 29] to investigate the $\bar{p}p \to \bar{\Lambda}\Lambda$ reaction. In this model, these reactions are considered within a coupled-channels framework, which allows one to take into account the initial and final state interactions in a rigorous way. The reaction proceeds via an exchange of appropriate mesons between p and $\bar{p}$ leading to the final baryon-antibaryon state. Also in Ref. [30] the meson-exchange picture was used to calculate the production rate of the charmed baryon $\Lambda_c^+(2940)$ in the $p\bar{p}$ annihilation at $\bar{P}ANDA$ energies.

The aim of this paper is to investigate the $\bar{p}p \to \bar{\Lambda}_c^- \Lambda_c^+$ reaction within a single-channel effective Lagrangian model (see, e.g., Refs. [31, 32]), where this reaction is described as a sum of t-channel D^0 and D^{*0} meson-exchange diagrams (see Fig. 1). The Λ_c^+ mass ($m_{\Lambda_c^+}$) is taken to be 2.286 GeV. The s- and u-channel resonance excitation diagrams are suppressed, as no resonance with energy in excess of 3.0 GeV having branching ratios for decay to the Λ_c^+ channel is known. Although, in some chiral coupled-channel studies [33, 34] the existence of narrow cryptoexotic

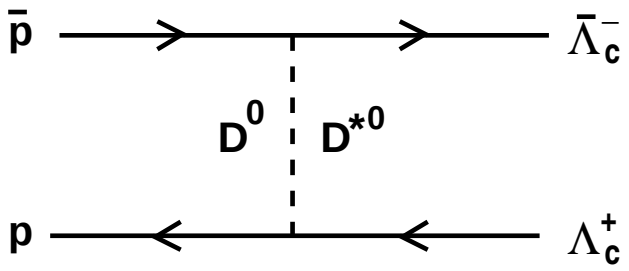

FIG. 1. (color online) Graphical representation of the model used to describe the $\bar{p}+p \to \bar{\Lambda}_c^- + \Lambda_c^+$ reaction. D^0 and D^{*0} in the intermediate line represent the exchanges of D^0 pseudoscalar and D^{*0} vector mesons, respectively.

baryon resonances with hidden charm has been predicted, these are confined in the mass range between 3 and 4 GeV/c^2 and are unlikely to contribute to the open charmed baryon production reaction. At the same time, the direct $p\bar{p}$ annihilation into $\bar{\Lambda}_c^-\Lambda_c^+$ via the contact diagrams is also suppressed due to the Okubo-Zweig-Iizuka condition.

In the next section, we present our formalism. The results and discussions of our work are given in Sec. III. Finally, the summary and the conclusions of this study are presented in Sec. IV.

II. FORMALISM

To evaluate various amplitudes for the processes shown in Fig. 1, we have used the effective Lagrangians at the charm baryon-meson-nucleon vertices, which are taken from Refs. [35–37]. For the D^0 meson [mass (m_{D^0}) = 1.865 GeV] exchange vertices we have

$$\mathcal{L}_{D^0BN} = ig_{BD^0N}\bar{\psi}_B i\gamma_5\psi_N\phi_{D^0} + H.c., \tag{1}$$

where ψ_B and ψ_N are the charmed baryon and nucleon (antinucleon) fields, respectively, and ϕ_{D^0} is the D^0 meson field. g_{BD^0N} in Eq. (1) represents the vertex coupling constant.

For the D^{*0} meson [mass ($m_{D^{*0}}$) = 2.007 GeV] exchange vertices, the effective Lagrangian is

$$\mathcal{L}_{D^{*0}BN} = g_{D^{*0}BN}\bar{\psi}_B\gamma_\mu\psi_N\theta^\mu_{D_{*0}} + \frac{f_{D^{*0}BN}}{4M}\bar{\psi}_B\sigma_{\mu\nu}\psi_N F^{\mu\nu}_{D^{*0}} + H.c., \tag{2}$$

where $\theta^\mu_{D_{*0}}$ is the vector meson field, with field strength tensor $F^{\mu\nu}_{D^{*0}} = \partial^\mu\theta^\nu_{D^{*0}} - \partial^\nu\theta^\mu_{D^{*0}}$. $\sigma_{\mu\nu}$ is the usual tensor operator. The vector and tensor couplings are defined by g and f, respectively, which were fixed in Refs. [36, 38, 39] by using SU(4) symmetry arguments in the description of the exclusive charmed hadron production in $\bar{D}N$ and DN scattering within a one-boson-exchange

picture. In our study we have adopted the values as given in Ref. [36] (see Table I). The same couplings were used for the vertices involving both the proton and the antiproton. It may be pointed out here that in the study presented in Ref. [30], the exchange of D^{*0} was not considered. As we shall show later on, this process dominates the $\Lambda_c^+\bar{\Lambda}_c^-$ production reaction in the $p\bar{p}$ annihilation even for beam momenta closer to the production threshold.

TABLE I. Coupling constants at the BD^0N and $BD^{*0}N$ vertices. These are taken from Ref. [36] where they are deduced from DN and $\bar{D}N$ scattering analysis. Here B represents the charmed baryon.

Vertex	$g_{DBN}/\sqrt{4\pi}$	$f_{DBN}/\sqrt{4\pi}$
ND^0B	3.943	–
$ND^{*0}B$	1.590	5.183

The off-shell behavior of the vertices is regulated by a monopole form factor (see, eg., Refs. [31, 32])

$$F_i(q_i) = \frac{\lambda_i^2 - m_{D_i}^2}{\lambda_i^2 - q_{D_i}^2}, \tag{3}$$

where q_{D_i} is the momentum of the ith exchanged meson with mass m_{D_i}. λ_i is the corresponding cutoff parameter, which governs the range of suppression of the contributions of high momenta carried out via the form factor. We chose a value of 3.0 GeV for λ_i at both the vertices. The same λ_i was also used in the monopole form factor employed in the studies presented in Refs. [25, 26]. It is of interest to note that a value of $\lambda = (2.89 \pm 0.04)$ was determined in Ref. [35] by a one-boson-exchange model fitting of the inclusive Λ_c^+ production cross section in the proton-proton collision measured by the R680 Collaboration at ISR [40]. Because the experimental data are not yet available for the reaction under investigation in this paper, we restrict ourselves to the choice of the form factor given by Eq. (3) with a λ_i value as mentioned above. This enables a meaningful comparison of our results with those of Refs. [25, 26].

For calculating the amplitudes, we require the propagators for the exchanged mesons. For the D^0 and D^{*0} mesons, the propagators are given by

$$G_{D^0}(q) = \frac{i}{q^2 - m_{D^0}^2}, \tag{4}$$

$$G_{D^{*0}}^{\mu\nu}(q) = -i\left(\frac{g^{\mu\nu} - q^\mu q^\nu/q^2}{q^2 - (m_{D^{*0}} - i\Gamma_{D^{*0}}/2)^2}\right). \tag{5}$$

In Eq. (5), $\Gamma_{D^{*0}}$ is the total width of the $D^{*0}(2007)$ meson which is about 2.0 MeV according to the latest particle data group estimate [41]. After having established the effective Lagrangians, coupling constants, and forms of the propagators, the amplitudes of various diagrams can be written by following the well-known Feynman rules. The signs of these amplitudes are fixed by those of the effective Lagrangians, the coupling constants, and the propagators as described above. These signs are not allowed to change anywhere in the calculations.

From the studies of the $\bar{p}p \to \bar{\Lambda}\Lambda$ reaction, it is known that there is a strong sensitivity of the calculated cross sections to the distortion effects in the initial and final states [28, 29, 42–50]. For the $\bar{\Lambda}_c^- \Lambda_c^+$ production channel also the magnitudes of the cross sections have been found [25] to depend very sensitively on the distortion effects.

For the $\bar{p}p$ initial state, the annihilation channel is almost as strong as the elastic scattering. This large depletion of the flux can be accounted for by introducing absorptive potentials that are used in optical model or in coupled-channels approaches [25, 28, 29, 46, 50]. In this work we do not employ such a detailed treatment. Instead, we use a procedure that was originated by Sopkovich [51]. In this method, the transition amplitude with distortion effects is written as

$$T^{\bar{p}p\to\bar{\Lambda}_c^-\Lambda_c^+} = \sqrt{\Omega^{\bar{p}p}}\, T_{Born}^{\bar{p}p\to\bar{\Lambda}_c^-\Lambda_c^+} \sqrt{\Omega^{\bar{\Lambda}_c^-\Lambda_c^+}} \tag{6}$$

where $T_{Born}^{\bar{p}p\to\bar{\Lambda}_c^-\Lambda_c^+}$ is the transition matrix calculated within the Born approximation and $\Omega^{\bar{p}p}$ and the $\Omega^{\bar{\Lambda}_c^-\Lambda_c^+}$ are the matrices describing the initial and final state elastic scattering, respectively. Their effect is to dampen the wave functions and hence the amplitudes. We, however, note that the derivation of this equation relies on the ideas of the high-energy eikonal model while we are dealing with low energies in the final channels. Nevertheless, it has been shown in Ref. [25] that, because of the strong absorption in the initial channel, the results turn out to be rather insensitive to the final state $\bar{\Lambda}_c^- \Lambda_c^+$ interactions. In fact, even if the final state interactions (FSIs) are ignored totally, the total cross sections do not change by more than 10%-15%. In order to keep the number of free parameters small, we, therefore, decided to fully neglect FSIs and concentrate only on the initial state interaction.

For the present purpose, we neglect the real part of the baryon-antibaryon interaction. Considering the $\bar{p}p$ initial state interaction, we describe the strong absorption by an imaginary potential of Gaussian shape with range parameter μ and strength V_0. By using the eikonal approximation, the corresponding attenuation integral can be evaluated in a closed form. Similar to Refs. [48, 51],

we obtain for $\Omega^{\bar{p}p}$

$$\Omega^{\bar{p}p} = exp[\frac{-\sqrt{\pi}EV_0}{\mu k} exp(-\mu^2 b^2)], \tag{7}$$

where b is the impact parameter of the $\bar{p}p$ collision. E and k are the center of mass energy and the wave vector of the particular channel, respectively. In our numerical calculations, we have used $V_0 = 0.8965$ GeV and $\mu = 0.3369$ GeV. With these values, the total cross sections are reasonably well described in the relevant energy region. For the impact parameter, we have taken a value of 0.327 GeV^{-1}. With these parameters, we are able to get cross sections for the $\bar{p}p \to \bar{\Lambda}\Lambda$ reaction in close agreement with the corresponding experimental data. Furthermore, they lead to cross sections for the $\bar{\Lambda}_c^- \Lambda_c^+$ production that are similar in magnitude to those reported in Ref. [25].

Although the parameters V_0 and μ may change with energy, we have made them global; that is, they remain the same at all the energies. Furthermore, the same parameters were used in the calculations of both the $\bar{p}p \to \bar{\Lambda}\Lambda$ and the $\bar{p}p \to \bar{\Lambda}_c^- \Lambda_c^+$ reactions. Thus, we have only three fixed parameters in our calculations of the initial state distortion effects.

III. RESULTS AND DISCUSSIONS

The formalism described above has been used first to describe the $\bar{p}p \to \bar{\Lambda}\Lambda$ reaction where experimental data are available for both near-threshold and far-from-threshold beam momenta. The aim is to check the parameters of our model (the coupling constants and those related to the distortion effects). In Fig. 2(a), we show the total cross section of this reaction for beam momenta closer to the reaction threshold (1.433 GeV/c) as a function of the excess energy (defined as $\sqrt{s} - m_{\bar{\Lambda}} - m_{\Lambda}$, with $\sqrt{s}$ being the invariant mass). In these calculations, we have considered the exchange of pseudoscalar $K(498)$ and pseudovector $K^*(892)$ mesons. A width of 48 MeV is taken in the denominator of the $K^*(892)$ propagator [Eq. (5)]. The effective Lagrangians for the baryon-meson-nucleon vertices were the same as those given by Eqs. (1) and (2). Assuming a complete SU(4) symmetry, the values of the vertex coupling constants were taken to be the same as those shown in Table 1. The parameters of the initial state distortion factor were also the same as described above. However, as in Refs. [28, 29], the cutoff parameter of the form factor in Eq. (3) was chosen to be 1.7 GeV due to the different mass regime of the exchanged mesons. The experimental data in Fig. 2(a) are taken from Refs. [52–54]. We note that there is a good overall agreement with the data for excess energies ranging between threshold and 100 MeV.

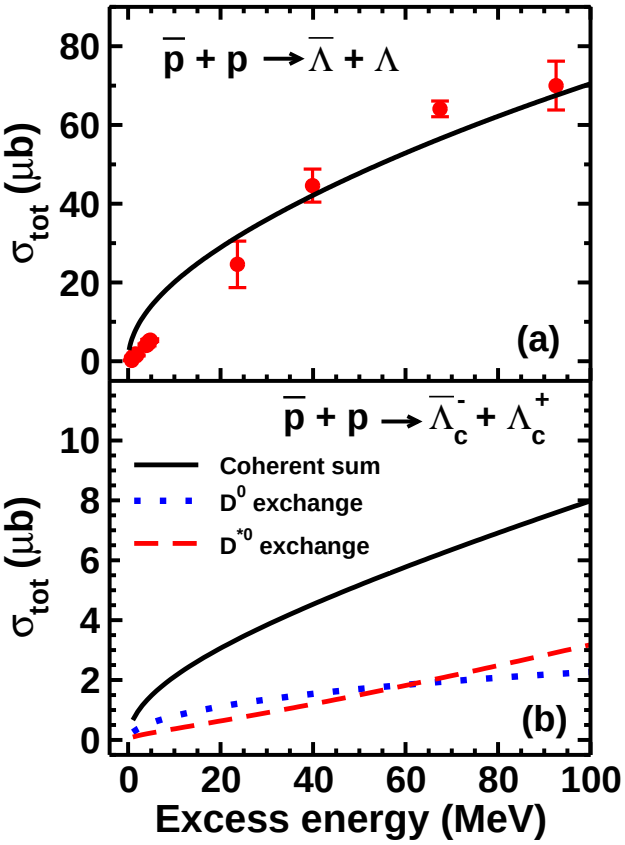

FIG. 2. (color online) Total cross section for the reactions $\bar{p}p \to \bar{\Lambda}\Lambda$ (a) and $\bar{p}p \to \bar{\Lambda}_c^- \Lambda_c^+$ (b) as a function of the excess energy. The experimental data in (a) are taken from [52–54]. In (b) the contributions of the D^0 and D^{*0} exchange processes are shown by dotted and dashed lines, respectively. The solid line represents their coherent sum.

In Fig. 2(b), our results for the $\bar{p}p \to \bar{\Lambda}_c^- \Lambda_c^+$ reaction are shown as a function of the corresponding excess energy (defined in this case as $\sqrt{s} - m_{\bar{\Lambda}_c^-} - m_{\Lambda_c^+}$). Because of the assumption of SU(4) symmetry, all the coupling constants were taken to be the same. Even the parameters involved in the $\bar{p}p$ distortion factors were the same. However, the cutoff parameter λ in this case was 3 GeV as discussed in the previous section. We notice that the magnitude of the cross section in Fig. 2(b) is smaller than that of Fig. 2(a) by nearly an order of magnitude. This is in agreement with the results obtained in the coupled-channel calculations presented in Ref. [25]. This difference has been attributed to the difference in the masses of the mesons involved in the corresponding propagators. We further note that very close to the threshold the contributions of the D^0 exchange are slightly larger than those of the D^{*0} exchange. However, with the increasing beam momentum, the situation reverses, and the D^{*0} exchange starts dominating the total cross section. The absolute

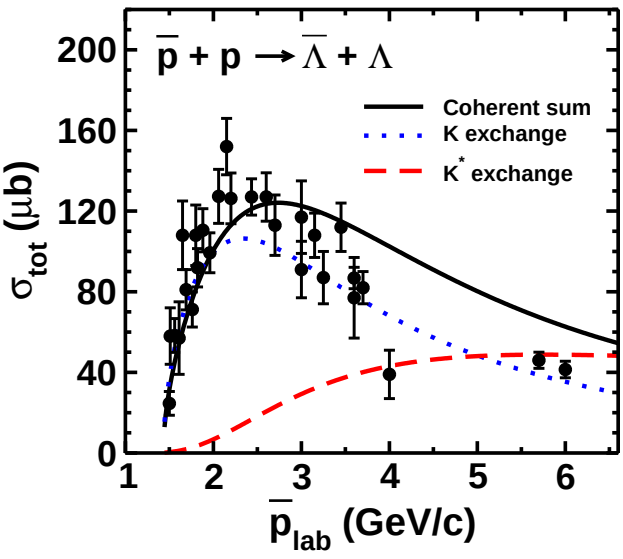

FIG. 3. (color online) Total cross section for the reaction $\bar{p}p \to \bar{\Lambda}\Lambda$ as a function of the antiproton beam momentum. The individual contributions of $K(494)$ and $K^*(892)$ exchange processes are shown by dotted and dashed lines, respectively. The solid line represents their coherent sum.

magnitudes of the cross sections in Fig. 2(b) are very similar to those of Ref. [25].

We next discuss our results at higher beam momenta. In Fig. 3, we compare the calculated total cross sections for the $\bar{p}p \to \bar{\Lambda}\Lambda$ with the corresponding experimental data that are available for incident $\bar{p}$ beam momenta ($\bar{p}_{lab}$) from near threshold to above 6 GeV/c [55]. It is clear that our calculations provide a reasonable description of the beam momentum dependence of the data. In this figure, we also show the individual contributions of the $K(494)$ and $K^*(892)$ meson-exchange processes. We note that for beam momenta near the threshold ($\bar{p}_{lab} < 2.0$ GeV/c) the K-exchange terms are dominant. However, for $\bar{p}_{lab}$ beyond this range the K^*-exchange process becomes important, and for $\bar{p}_{lab} > 6.0$ GeV/c it contributes most to the total cross section. This result is in agreement with the observations made in several previous studies (see, e.g., Ref. [43] and the references of the older works cited there).

Some disagreement seen in Fig. 3 between the theory and the data for $\bar{p}_{lab}$ beyond ≥ 4.0 GeV/c could be an indication of the increasing importance of larger mass strange meson contributions at higher beam momenta. It has been noted in Ref. [43] that, at higher beam energies, the $K_2^*(1430)$ meson-exchange process becomes crucial, as it interferes destructively with the $K^*(892)$ terms. In any case, since we are mainly interested in the overall mechanism of the production of the flavored baryon-antibaryon pair in the $\bar{p}p$ annihilation reaction, and also since there are large uncertainties

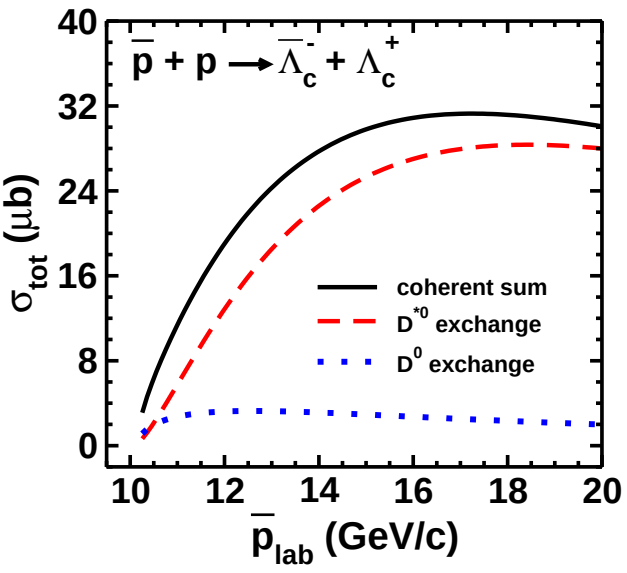

FIG. 4. (color online) Total cross section for the reaction $\bar{p}p \to \bar{\Lambda}_c^- \Lambda_c^+$ as a function of the antiproton beam momentum. The contributions of the D^0 and D^{*0} exchange processes are shown by dotted and dashed lines, respectively. The solid line represents their coherent sum.

in the data, we refrain from attempting a detailed fit to the data.

For the charm baryon production reaction, we investigate the role of various meson-exchange processes at higher beam momenta in Fig. 4. In this figure, we show the total cross sections for the $\bar{p}p \to \bar{\Lambda}_c^- \Lambda_c^+$ reaction for $\bar{p}_{lab}$ varying in the range of threshold to 20 GeV/c. First we note that the cross sections peak around $\bar{p}_{lab}$ of 15 GeV/c, and thereafter they decrease gradually. We further see that the vector meson (D^{*0}) exchange process dominates the cross section except for very-close-to-threshold beam momenta. For $\bar{p}_{lab} \geq 15$ GeV/c, the D^0-exchange contributions are nearly an order of magnitude smaller than those of the D^{*0}-exchange. However, it is also clear in this figure that, even though for $\bar{p}$ beam momenta away from the threshold the individual contributions of the D^0 exchange processes are small, they are not negligible, as they contribute significantly through the interference terms which are constructive for this case.

To explore the origin of the domination of the D^{*0} exchange contributions, we note the relative strong coupling to the vector meson vertices, particularly for the tensor coupling term. As can be seen from Table I, the ratio of tensor to vector coupling is 3.26. This analogous to the large tensor coupling for the ρ meson in the one-boson-exchange models of the NN interaction [56], where the tensor to vector ratio is even larger (6.1). In Fig. 5, we show the individual contributions of the vector and tensor terms to the total D^{*0} exchange cross section. Clearly, the tensor coupling

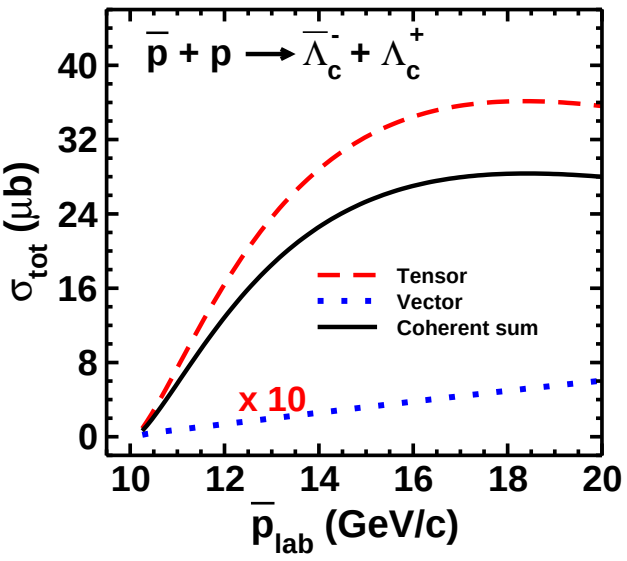

FIG. 5. (color online) Contributions of the vector and tensor coupling terms to the D^{*0} exchange cross sections for the $\bar{p}p \to \bar{\Lambda}_c^- \Lambda_c^+$ reaction as a function of the antiproton beam momentum. The contributions of the tensor and vector terms are shown by the dashed and dotted lines, respectively. The solid line represents their coherent sum.

terms make the dominant contribution to the D^{*0} exchange part of the total cross section. The interference of vector and tensor coupling terms is destructive as the total D^{*0} cross sections are lower than the individual contribution of the tensor term. At the effective Lagrangian level, the strong tensor contribution is associated with the additional momentum dependence induced by the derivative coupling in the tensor interaction [see Eq. (2)].

A comparison of our results with those of the previous studies would be of interest in the planning of the future experiments for the charm baryon production at the $\bar{P}ANDA$ facility. For this purpose, we chose the $\bar{p}_{lab}$ of 15 GeV/c. For this beam momentum, results for the total cross section of the $\bar{p}p \to \bar{\Lambda}_c^- \Lambda_c^+$ reaction have been reported in Refs. [22, 24, 27], which are approximately 100, 1.2, and 60 nb, respectively. These values are drastically lower than the corresponding cross section predicted in our study. On the other hand, our results are in close agreement with those of Refs. [25, 26] even though they have given predictions for the cross section only for near-threshold beam momenta. Thus, even when considering the variation in values predicted in our model due to the unconstraint initial and final state distortions and the ansatz of the form factor at various vertices, the differences between our cross sections and those of Refs. [22, 24, 27] are substantial for beam momenta relevant to the $\bar{P}ANDA$ experiment.

The differential cross section (DCS) provides more valuable information about the reaction mechanism. The DCS includes terms that weigh the interference terms of various components of the amplitude with angles of the measured outgoing particle. Therefore, the structure of the interference terms could highlight the contributions of different meson exchanges in different angular regions. In Fig. 6, we show our results for differential cross sections at the beam momenta of 10.25, 12.25, and 16.25 GeV/c. For all three beam momenta, the cross sections are peaked in the forward directions. By looking at the relative contributions of the D^0 and D^{*0} exchange processes that are shown by the dotted and dashed lines, respectively, their strongly different characteristics in different angular regions become very apparent. While the D^0 exchange terms are large in the backward directions, those of the D^{*0} exchange are forward peaked. We also note that, while there is destructive interference among the two exchange terms at back angles, they are strongly constructive in the forward directions. Even though the individual D^0 exchange contributions are small at the forward angles, they play an important role in the total cross sections through the interference terms.

IV. SUMMARY AND CONCLUSIONS

In summary, we studied the $\bar{p}p \to \bar{\Lambda}_c^- \Lambda_c^+$ reaction using a phenomenological effective Lagrangian model that involves the meson-baryon degree of freedom. The detailed dynamics of the process is accounted for by the t-channel D^0 and D^{*0} exchange diagrams, while largely phenomenological initial and final state interactions have been used to account for the distortion effects. The coupling constants at various vertices have been taken from the DN and $\bar{D}N$ scattering studies reported in Refs. [36, 38, 39]. The off-shell corrections at the vertices are accounted for by introducing monopole form factors with a cutoff parameter of 3.0 GeV, which was taken to the same for all the cases. This ansatz for the form factor and the value of the cutoff parameter λ have been checked by fitting the data on the $pp \to \Lambda_c^+ X$ reaction measured by the ISR Collaboration [40] in Ref. [35]. A further check on the input parameters of our model is performed by taking over the same coupling constants and the form factor to describe the data on $\bar{p}p \to \bar{\Lambda}\Lambda$ reaction under the assumption of SU(4) symmetry. Of course, the value of the cutoff parameter cannot be taken over, as the masses of the exchanged mesons for this reaction are much smaller. We used a λ of 1.7 GeV for this case in line with the choice of Refs. [28, 29]. Our calculations provide a good description of the data for this reaction.

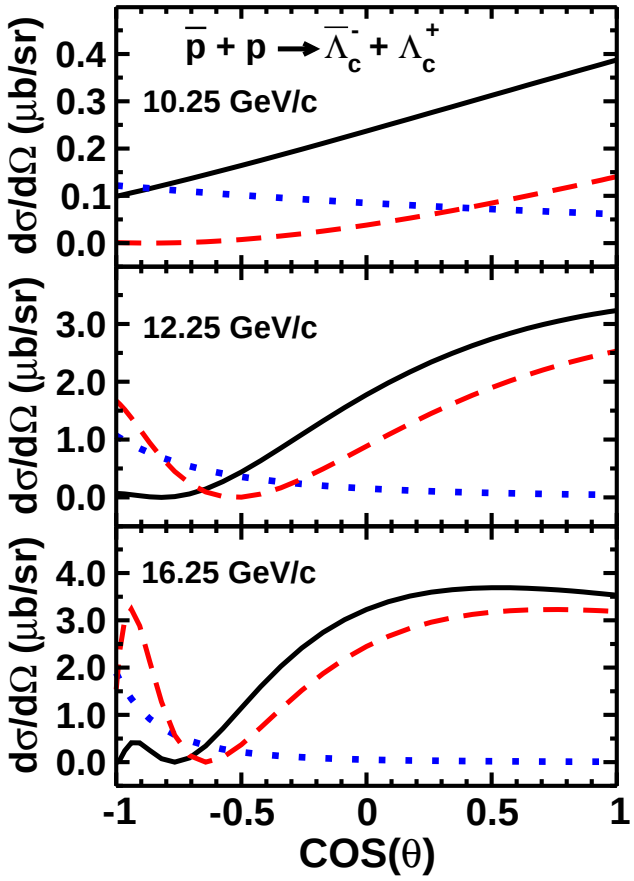

FIG. 6. (color online) Differential cross sections for the $\bar{p}p \rightarrow \bar{\Lambda}_c^- \Lambda_c^+$ reaction at the beam momenta of 10.25, 12.25, and 16.25 GeV/c as indicated in the figure. Contributions of the D^0 and D^{*0} exchange processes are shown by dotted and dashed lines, respectively, in each case. The solid lines represent their coherent sum.

The total cross section for the $\bar{p}p \rightarrow \bar{\Lambda}_c^- \Lambda_c^+$ vary between 1 and 8 μb at near-threshold beam momenta (excess energy between 1 and 100 MeV). This value agrees with that reported in the coupled-channels meson-exchange model calculations of Refs. [25, 26]. For higher beam momenta, the cross sections are larger. They peak around a $\bar{p}_{lab}$ of 15 GeV/c with a peak value of around 30 μ b. This value is drastically larger than the cross sections for this reaction predicted in previous calculations. Since these earlier calculations have used different types of models, which by and large invoke the quark degrees of freedom in their calculations, it is difficult to locate the reason for the large difference between them and our results. This will be understood when the $\bar{P}ANDA$ experiment performs these measurements once the FAIR facility is operational. If the cross sections are as large as predicted in our calculations as well as in those of Refs. [25, 26], it

would be relatively easy to measure them at the $\bar{P}ANDA$ experiment.

We noted that the vector meson (D^{*0}) exchange terms dominate the cross sections for all beam momenta except for those very close to the production threshold. The reasons for the large strength of this exchange process are the strong tensor coupling of the vector mesons (similar to the large tensor coupling of the ρ meson in NN interactions), and the additional momentum dependence introduced by the derivative part of the corresponding interaction. Although, except for the very-close-to-threshold beam momenta, the individual contributions of the D^0 exchange terms are relatively weak, they contribute significantly through the interference terms.

We found that different meson-exchange processes contribute in different angular reasons of the differential cross sections, which are generally forward peaked both at lower as well as higher beam momenta. It was noted that while the D^0 exchange terms dominate in the backward directions, D^{*0} exchange processes are relatively large in the forward angular region. The constructive interference between these two exchange processes leads to more forward peaking of the cross sections. On the other hand, D^0 exchange terms alone yield backward-peaked differential cross sections.

The initial and final state interactions are the important ingredients of our model. We treat them within an eikonal approximation-based phenomenological method. Generally, the parameters of this model are constrained by fitting to the experimental data. Because of the lack of any experimental information, it has not been possible to test our model thoroughly. Therefore, there may be some uncertainty in the absolute magnitudes of our cross sections. Nevertheless, we reproduce the data for the $\bar{\Lambda}\Lambda$ production channel, and our near-threshold cross sections for the $\bar{\Lambda}_c^- \Lambda_c^+$ production are very close to those of Refs. [25, 26], where distortion effects have been treated more rigorously within a coupled-channels approach. Therefore, the large cross sections obtained in our calculations at larger beam momenta as compared to those of previous authors are robust and can help in planning of the experiments to measure this channel at the $\bar{P}ANDA$ facility.

V. ACKNOWLEDGMENTS

This work has been supported by the German Research Foundation (DFG) under Grant No. Le439/8-2 and Helmholtz International Center (HIC) for FAIR and the Council of Scientific and

Industrial Research (CSIR), India.

[1] N. Isgur and M. B. Wise, Phys. Lett. B **232**, 113 (1989).

[2] M. Neubert, Phys. Rep. **245**, 259 (1994).

[3] A. G. Grozin, arXiv:hep-ph/9908366.

[4] A. V. Manohar and M. B. Wise, *Cambridge Monographs on Particle Physics, Nuclear Physics and Cosmology*, (Cambridge University Press, Cambridge, England, 2000), Vol. 10.

[5] J. G. Körner, M. Krämer, and D. Pirjol, Prog. Part. Nucl. Phys. **33**, 787 (1994).

[6] J. Aubert *et al*., Phys. Rev. Lett. **33**, 1404 (1974).

[7] J. Augustin *et al*., Phys. Rev. Lett. **33**, 1406 (1974).

[8] E. S. Swanson, Phys. Rep. 429, 243 (2006)

[9] S. Godfrey and S. L. Olsen, Annu. Rev. Nucl. Part. Sci., **58**, 51 (2008).

[10] I. Katkov,arXiv:hep-ex/0309043.

[11] M. Steder, Report No DESY-THESIS-2008-023.

[12] V. Santoro (*BABAR* Collaboration), arXiv:1311.7531

[13] M. Uchida (Belle Collaboration), Few-Body Syst. **54**, 947 (2013).

[14] Rong-Gang Ping (BESIII Collaboration), Nucl.Phys. B, Proc.Suppl. **234**, 133 (2013).

[15] G. T. Bodwin, arXiv:1208.5506.

[16] E. Cazzoli, A. Cnops, P. Connolly, R. Louttit, M. Murtagh, R. Palmer, N. Samios, T. Tso, and H. Williams, Phys. Rev. Lett. 34, 1125 (1975).

[17] M.S. Dubrovin (CLEO Collaboration), hep-ex/0305006.

[18] V. Ziegler (*BABAR* Collaboration), AIP Conf.Proc. 1374, 577 (2011), and references therein.

[19] Y. Kato (Belle Collaboration), Proc. Sci. Hadron2013 (2014), 053, and references therein.

[20] U. Wiedner, Prog. Part. Nucl. Phys. **66**, 477 (2011).

[21] P. Kroll, B. Quadder, and W. Schweiger, Nucl. Phys. B **316**, 373 (1989).

[22] A. B. Kaidalov and P. E. Volkovitsky, Z. Phys. C **63**, 517 (1994).

[23] A. I. Titov and B. Kämpfer, Phys. Rev. C **78**, 025201 (2008).

[24] A. T. Goritschnig, P. Kroll, and W. Schweiger, Eur. Phys. J. A **42**, 43 (2009).

[25] J. Haidenbauer, and G. Krein, Phys. Lett. B **678**, 314 (2010).

[26] J. Haidenbauer, and G. Krein, Few-Body Syst. **50**, 183 (2011).

[27] A. Khodjamirian, Ch. Klein, Th. Mannel, and Y.-M. Wang, Eur. Phys. J. A **48**, 31 (2012).

[28] J. Haidenbauer, T. Hippchen, K. Holinde, B. Holzenkamp, V. Mull and J. Speth, Phys. Rev. C **45**, 931 (1992).

[29] J. Haidenbauer, K. Holinde, V. Mull and J. Speth, Phys. Rev. C **46**, 2158 (1992).

[30] Jun He, Zhen Ouyang, Xiang Liu, and Xue-Qian Li, Phys. Rev. D **84**, 114010 (2011).

[31] R. Shyam, Phys. Rev. C **60**, 055213 (1999).

[32] R. Shyam and U. Mosel, Phys. Rev. C **67**, 065202 (2003).

[33] J. Hofmann and M. F. M. Lutz, Nucl. Phys. **A 763**, 90 (2005).

[34] M. F. M. Lutz and J. Hofmann, Int. J. Mod. Phys. A **21**, 5496 (2006).

[35] T. J. Hobbs, J. T. Londergan, and W. Melnitchouk, Phys. Rev. D 89, 074008 (2014)

[36] J. Haidenbauer, G. Krein, U.-G. Meissner, and L. Tolos, Eur. Phys. J. A **47**, 18 (2011).

[37] A. Müller-Groeling, K. Holinde, and J. Speth, Nucl. Phys. A **513**, 557 (1990).

[38] J. Haidenbauer, G. Krein, U.-G. Meissner, and A. Sibirtsev, Eur. Phys. J. A **33**, 107 (2007).

[39] J. Haidenbauer, G. Krein, U.-G. Meissner, and A. Sibirtsev, Eur. Phys. J. A **37**, 55 (2008).

[40] P. Chauvat *et al.*, Phys. Lett. B **199**, 304 (1987).

[41] J. Beringer *et al*. (Particle Data Group), Phys. Rev. D **86**, 010001 (2012).

[42] H. Genz and S. Tatur, Phys. Rev. D **30**, 63 (1984).

[43] F. Tabakin and R. A. Eisenstein, Phys. Rev. C **31**, 1857 (1985).

[44] P. Kroll and W. Schweiger, Nucl. Phys. A **474**, 608 (1987).

[45] M. Burkardt and M. Dillig, Phys. Rev. C **37**, 1362 (1988).

[46] M. Kohono and W. Weise, Nucl. Phys. A **454**, 429 (1986).

[47] G. Brix, H. Genz and S. Tatur, Phys. Rev. D **39**, 2054 (1989).

[48] W. Roberts, Z. Phys. C **49**, 633 (1991).

[49] F. Tabakin, R. A. Eisenstein, and Y. Lu, Phys. Rev. C **44**, 1749 (1991).

[50] M. A. Alberg, E. M. Henley, L. Wilets, P. D. Kunz, Nucl. Phys. A **560**, 365 (1993).

[51] N. J. Sopkovich, Nuovo Cimento **26**, 186 (1962).

[52] P. D. Barns et al., Phys. Lett. B **229**,432 (1989).

[53] P. D. Barns et al., Nucl. Phys. A **526**, 575 (1991).

[54] P. D. Barns et al., Phys. Rev. C **54**, 1877 (1996).

[55] V. Flaminio, W. G. Moorhead, D. R. O. Morrissson, and N. Rivoire, CERN Report No. CERN-HERA-84-01, 1984.

[56] R. Machleidt, K. Holinde, and C. Elster, Phys. Rep. **149**, 1 (1987).